A general mechanism for signal propagation in the nicotinic acetylcholine receptor family

Ana Sofia F. Oliveira,[a,b] Christopher J. Edsall[c], Christopher J. Woods,[b,c] Phil Bates,[d,e] Gerardo Viedma Nunez,[e] Susan Wonnacott,[f] Isabel Bermudez,[g] Giovanni Ciccotti,[h,i,j] Timothy Gallagher,[b] Richard B. Sessions[a*] and Adrian J. Mulholland[b*]

*E-mail: r.sessions@bristol.ac.uk adrian.mulholland@bristol.ac.uk

[a] School of Biochemistry, University of Bristol, Bristol BS8 1DT (United Kingdom)

[b] Centre for Computational Chemistry, School of Chemistry, University of Bristol, Bristol BS8 1TS (United Kingdom)

[c] Research Software Engineering, Advanced Computing Research Centre, University of Bristol, Bristol BS1 5QD (United Kingdom)

[d] Department of Computer Science, Faculty of Engineering, University of Bristol, Bristol BS8 1TR (United Kingdom)

[e] Oracle Corporation, Oracle Cloud Development Centre, Bristol BS2 2JJ (United Kingdom)

[f] Department of Biology and Biochemistry, University of Bath, Bath BA2 7AY (United Kingdom)

[g] Department of Biological and Medical Sciences, Oxford Brookes University, Oxford OX30BP, UK

[h] Institute for Applied Computing "Mauro Picone" (IAC), CNR, Via dei Taurini 19, 00185 Rome, Italy

[i] School of Physics, University College of Dublin UCD-Belfield, Dublin 4, Ireland

[j] Università di Roma La Sapienza, Ple. A. Moro 5, 00185 Roma, Italy

Abstract

Nicotinic acetylcholine receptors (nAChRs) modulate synaptic activity in the central nervous system. The α7 subtype, in particular, has attracted considerable interest in drug discovery as a target for several conditions, including Alzheimer's disease and schizophrenia. Identifying agonist-induced structural changes underlying nAChR activation is fundamentally important for understanding biological function and rational drug design. Here, extensive equilibrium and nonequilibrium molecular dynamics simulations, enabled by cloud-based high-performance computing, reveal the molecular mechanism by which structural changes induced by agonist unbinding are transmitted within the human α7 nAChR. The simulations reveal the sequence of coupled structural changes involved in driving conformational change responsible for biological function. Comparison with simulations of the α4β2 nAChR subtype identifies

features of the dynamical architecture common to both receptors, suggesting a general structural mechanism for signal propagation in this important family of receptors.

Nicotinic acetylcholine receptors (nAChR) are prototypical members of the Cys loop pentameric ligand-gated ion channel (pLGICs) family, which also includes the $GABA_A$ and 5-HT3 receptors.[1-3] In the peripheral nervous system, nAChRs mediate fast excitatory synaptic signalling whereas in the brain they mostly modulate the synaptic signalling of a wide range of neurotransmitters.[4] Neuronal nAChRs expressed in the CNS are putative targets for the treatment of a variety of neurodegenerative diseases, neurodevelopmental disorders, pain and addiction[5], and analogous nAChRs in the insect CNS are targets for neonicotinoid pesticides.[6] The α7 subtype is one of most abundant nAChRs subtypes in the mammalian CNS[5], attracting considerable interest for drug discovery due to its role in cognition, attention, memory and sensory processing.[7] α7 nAChR dysfunction is implicated in disorders such as Alzheimer's and Parkinson's diseases and schizophrenia.[5]

There are many nAChR subtypes, distinguished by their specific combination of five subunits[1-3, 8]. Despite differences in sequence (Figure S1), all subunits share the same basic architecture (Figure 1), consisting of a N-terminal extracellular domain (ECD), a transmembrane domain (TMD), a variable cytoplasmic domain (ICD) and a short extracellular C-terminal domain.[1-3] The structures of nAChRs (and other pLGICs) have been revealed by cryo-electron microscopy[9-11] and X-ray crystallography[12]. The agonist-binding pockets are located in the ECDs at the interface between two neighbouring subunits (Figure 1). The α7 receptor subtype is unusual in being formed of five identical α7 subunits symmetrically arranged around a central ion channel[1-3] and thus presents five equivalent binding pockets, lined by several highly conserved aromatic residues.[13]

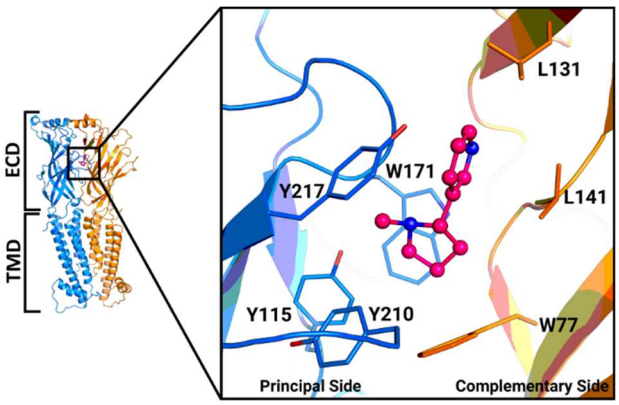

Figure 1. **Close-up view of the ligand-binding pocket of human α7 nAChR**. A model for the α7 subtype was built using as a template the α4 subunit of the human α4β2 nAChR[12]. Nicotine was modelled in two nonconsecutive binding pockets, similar to what is observed in the human α4β2 nAChR structure[12] (see Supporting Information). Nicotine is represented in balls-and-sticks.

Binding of acetylcholine (and other agonists such as nicotine) leads to opening of the ion channel, causing a flow of positive ions across the membrane, triggering depolarisation and signalling mechanisms.[2,14] Several regions at ECD-TMD interface have been shown to be essential for linking the agonist binding site to the channel gate (e.g.[15-25]), namely the β10-M1 region (which covalently links the ECD and TMD) and the Cys, F and β1-β2 loops, which are in direct contact with the M2-M3 linker, a well-established gating control element.[20,22,26-30] However, while the application of a variety of experimental approaches has led to a greater insight into the function of nAChR, the conformational changes induced by agonist binding/unbinding and how those are communicated to the ion channel remain poorly defined. Answering this question requires knowledge of the dynamics of the protein and the temporal evolution of the conformational changes that take place upon ligand (un)binding. Biomolecular simulations have the potential to investigate these questions[31], but face serious challenges associated with the large size of the systems and timescales involved; we show here that these can be overcome by the use of cloud-based high-performance computing (HPC) and by advanced, nonequilibrium molecular dynamics (MD) simulations, complementing standard equilibrium MD. In previous work on human α4β2 nAChR[32], we demonstrated how a combination of equilibrium and nonequilibrium MD simulations identified the structural motifs involved in signal propagation upon nicotine unbinding and the sequence of the events associated with the first steps of this process. Here, we have applied this novel approach to the human α7 nAChR, using cloud-based nonequilibrium simulations to complement more traditional high-performance computing to achieve long timescales and extensive sampling. We identify the dynamic structural mechanism of receptor response to nicotine and, by comparison with the human α4β2 nAChR, we find a common signal propagation pathway in nAChRs, which may generally apply to pLGICs.

Extensive equilibrium MD simulations (totalling 10 μs), with and without nicotine bound, were performed to identify the conformational changes induced by the ligand in the human α7 nAChR receptor. These simulations show that nicotine induces conformational changes in the binding pocket region, namely in loop B and C and also at the ECD:TMD interface, namely in the Cys and F loops and in the M2-M3 linker (Figures S10-S13). These results correlate well with the experimental evidence indicating that loop B, C and F have a role in binding (e.g.[33,34]) and agonist affinity[35,36]. Structural changes are also observed in the second layer of residues surrounding the binding site, mainly in the extracellular selectivity filter region (Figure S14). Note that a despite some differences in amplitude, similar structural changes are observed between the two binding pockets (Figure S10-S11). Although loop F has been shown to be essential for binding[13], its role in signal propagation remains elusive.[37,38] In our nicotine-bound equilibrium simulations, the motions of the upper part of loop F (residues D186-Y190) are coupled to the movements of the ECDs (right-side panels in Figure S15-S16), mostly to the binding-site region (loops B, C and loop D). The dynamics of the lower part of loop F (residues P192-W196) are highly correlated with the ECDs (namely the loops A, B, C and D in the binding pockets and the Cys loop at the interface between domains) and the TMDs (namely transmembrane helices M1, M2 and M3 and the M2-M3 linker).

When nicotine is present in the binding pockets, the dynamics of the M2-M3 linker is highly correlated not only with transmembrane helices 1, 2 and 3 but also with the Cys loop and some of the structural motifs forming the binding pockets, namely loops A, B and C (Figure S17). Several experimental studies have shown that mutations in the M2-M3 linker alter channel gating and disrupt the communication between domains in nAChRs (e.g.[20,22,26,28-30,39,40]) and in other pLGICs (e.g.[27,41-45]).

These simulations of human α7 nAChR, combined with results for the human α4β2 nAChR[32], reveal a common pattern of nicotine-induced structural rearrangements. Despite the differences in sequences between the two receptors, including differences in the Cys, B and C loops and M2-M3 linker (Figures S1-S2), similar conformational changes are observed in these structural elements. The largest difference in behaviour between the subtypes occurs in loop A, which shows a significant rearrangement in α7 but not in the α4β2 subtype.

Here, a set of 450 nonequilibrium simulations without nicotine was performed to identify the signal propagation pathway in the α7 nAChR. The equilibrium and nonequilibrium simulations are complementary approaches. The former allows for identification of the agonist-induced conformational changes (after hundreds of nanoseconds), while the latter allows for the determination of the order of the events associated with signal propagation and interdomain communication.

In all nonequilibrium simulations performed, both nicotine molecules were instantaneously annihilated. These simulations reveal the response of the system to this perturbation, specifically showing the mechanical and dynamical coupling between structural elements involved in the response (Figures 2, S20-S22 and Movie 1). Note that the nonequilibrium simulations performed here do not imply free energy calculations (e.g.[46-49]). In this case, it is the introduction of a perturbation that forces the system out of equilibrium. The Kubo-Onsager approach pioneered by Ciccotti[50-52] was used to compute the response of the receptor to nicotine removal (Figures S18-S19), by comparing the differences in the evolution of the simulations with and without nicotine, averaged over large numbers of simulations. The subtraction approach, and averaging over multiple (450) short simulations, allows conformational changes and their temporal sequence to be identified and their statistical significance to be determined. These nonequilibrium simulations are not intended to model the physical process of ligand (un)binding, nor the transition between states and, due to the artificial nature of the perturbation, the timescales observed for the response of the receptor do not represent the biological timescales.[32] It is also important to note that, due to the short timescale of the nonequilibrium simulations (5 ns), the observed deviations reflect only the first steps in the interdomain communication mechanism (Figures S20-S21).

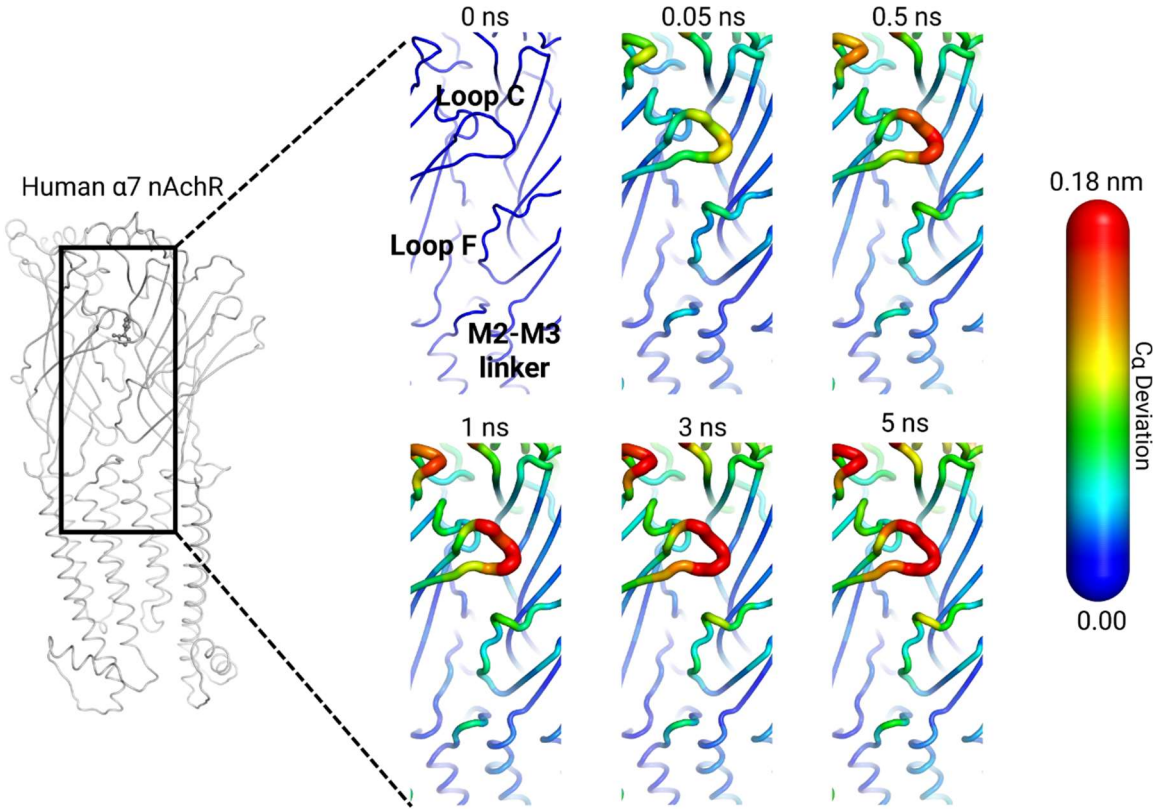

Figure 2- Signal propagation pathway from the ECD to the TMD in the α7 nAChR. Average Cα-positional deviation at times 0, 0.05, 0.5, 1, 3 and 5 ns following nicotine annihilation from the first binding pocket. The Cα deviations between the simulations with and without nicotine were determined for each residue, and the final values were averaged over the 450 pairs of simulations (Figure S18-S19). The Cα average deviations are mapped onto the average structure for the system without nicotine using the colour scheme in the scale on the right.

The 450 nonequilibrium simulations were performed in five days using the Oracle Cloud and 100 compute instances managed via cluster-in-the-cloud (https://cluster-in-the-cloud.readthedocs.io and https://doi.org/10.5281/zenodo.3246253). Profiling cloud versus on-premises computing suggested that these simulations would have taken around three months on shared local HPC resources. This demonstrates the rapid turnaround and throughput of high-end scientific computation (in this case intensive, physics-based atomistic MD simulations) that is now possible using such cloud services. The approach here combines strengths of traditional HPC (for equilibrium simulations) with the cloud (for nonequilibirum simulations).

The nonequilibrium simulations show that signal transmission in the α7 receptor starts in the binding pocket region, in loop C, and it then propagates to loop F and finally to the TMDs (Figure 2). Unsurprisingly, loop C (residues S206-Y217) is the first region to respond to ligand removal, and after 0.05 ns, some conformational rearrangements are already observed in this region. Over the next few nanoseconds, gradual and cumulative conformational changes propagate to the top (residues D186-Y190) and then to the lower part of loop F (residues P192-W196) and afterwards to the TMDs via the M2-M3 linker (residues T286-V290) (Figures 2, S20-S21 and Movie 1). Note that the two binding pockets show similar responses to nicotine annihilation, with the same order of events observed for each (Figures S18-S19). All the structural motifs identified here have been shown experimentally to be involved in ligand binding and signal transduction: Loop C is important for binding (e.g.[33,34]), contributing to binding the ammonium group of the agonists[13,53]; Loop F plays a role in ligand binding affinity,

and specificity[13]; and the M2-M3 linker is essential for channel gating and communication between domains (e.g.[22,26-30,39-45]), and insertions/deletions of residues in this region directly affect the open-channel lifetime.[30]

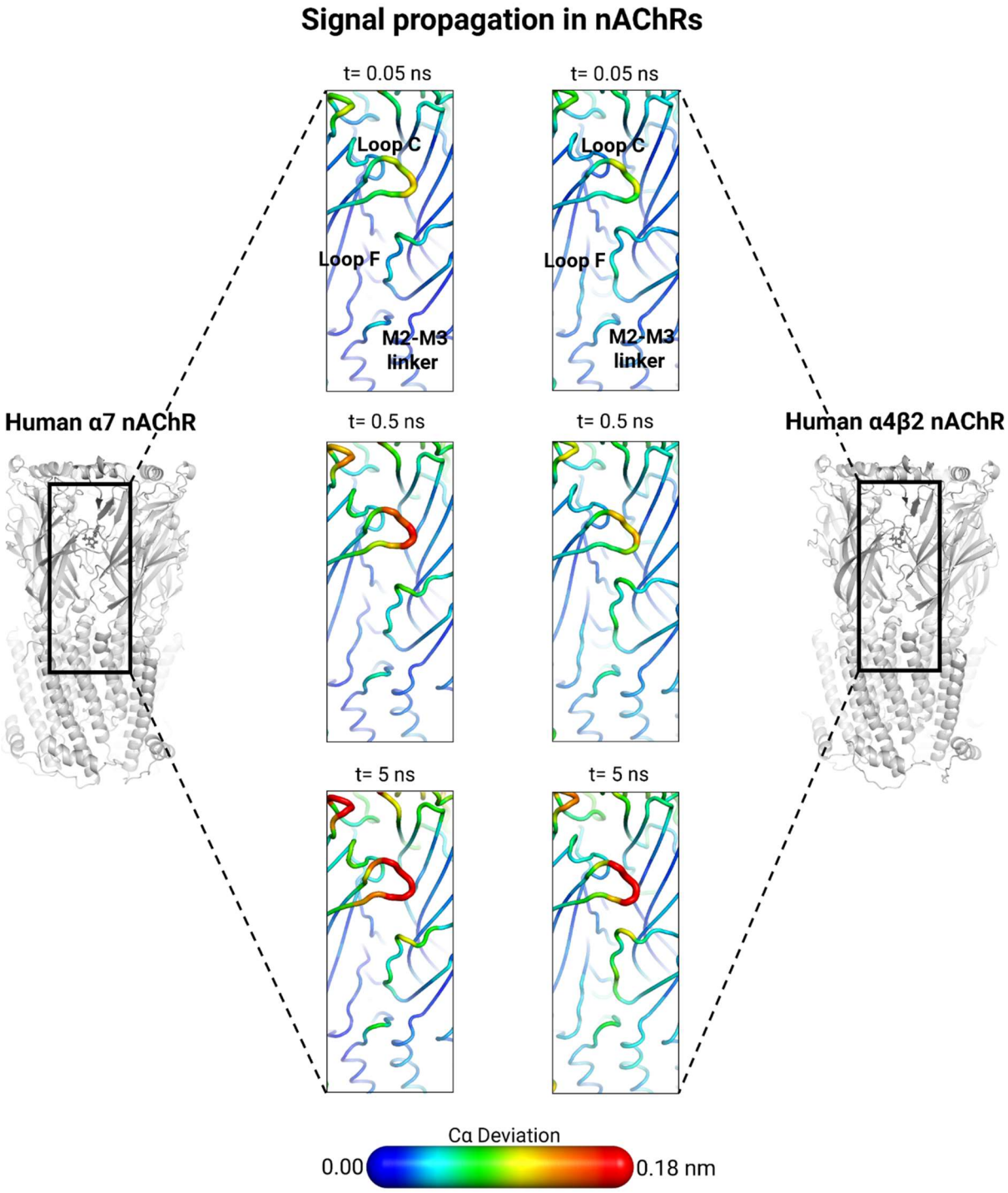

Figure 3- The ECD:TMD signal propagation pathway in human α7 and α4β2 nAChRs. The deviations for the α4β2 nAChR are taken from[32]. Note that although the apparent rate of propagation is different, the sequence of conformational changes associated with the initial steps of signal propagation is the same for both subtypes, i.e. the structural elements involved (loops C, F and M2-M3 linker), and the sequence of structural changes, are the same.

The signal propagation pathway observed here for the α7 nAChR is remarkably similar to that of the α4β2 nAChR.[32] The structural motifs involved in the signal transmission and the sequence of changes are the same between the two subtypes (Figure 3 and Movie 2). This supports the idea that, despite differences in sequence[13,54], all family members share a common communication mechanism. Our simulations show differences in the rate of propagation, which may relate to differences in function and response between receptor subtypes. All known pLGICs have a similar molecular architecture[1-3] and it has been shown experimentally that all of the structural elements identified here (loops C, F, Cys and the M2-M3 linker) are important not only in nAChR (e.g.[15,20,22,26,28,30,39,40]) but also in other homologous receptors (e.g.[37,38,55-58]). Furthermore, it is also known that chimeric pLGICs formed by modular combinations of different ECDs and TMDs are still functional.[21,59,60]

Our findings identify a general mechanism for communication within this receptor family: the structural rearrangements associated with signal propagation start in loop C and are subsequently transmitted, gradually and cumulatively, to loop F, and then to the TMDs via the M2-M3 linker. This mechanism is consistent with experimental data and provides a molecular-level rationalisation of those data. This dynamic mechanism of signal propagation not only confirms the involvement of specific structural motifs but also shows, for the first time, the complex contribution of Loop F to signal propagation. It should also assist in the design of agonists or allosteric modulators to target nAChRs and other biomedically relevant pLGICs. The approach used here, combining extensive equilibrium and nonequilibrium simulations, is a valuable tool to study conformational changes in allosteric proteins.

Supporting Information. [Detailed description of the methods, conformational stability of the α7 nAChR, dynamic behaviour of the nicotine ligands, nicotine-induced conformational changes, nonequilibrium analysis]

Acknowledgements

We thank EPSRC (EP/N024117/1, EP/N018591/1 and EP/M022609/1) for support. The equilibrium simulations were carried out using the computational facilities of the Advanced Computing Research Centre, University of Bristol (http://www.bris.ac.uk/acrc). All nonequilibrium simulations were performed in the Oracle Public Cloud Infrastructure (https://cloud.oracle.com/en_US/iaas). This work received generous support from the Oracle Cloud Innovation Accelerator (https://www.oracle.com/industries/education-and-research/innovation-accelerator/) to enable data processing and molecular dynamics simulations using Oracle's high-performance public cloud infrastructure (https://cloud.oracle.com/en_US/cloud-infrastructure). We also thank Achieve Life Sciences for useful discussion and support.

Author Contributions

Conceptualization/design of the work: Ana Sofia F. Oliveira, Richard B. Sessions and Adrian J. Mulholland; Software creation: Ana Sofia F. Oliveira, Christopher J. Edsall, Christopher J. Woods, Phil Bates and Gerardo Viedma Nunez; Acquisition and analysis of the data: Ana Sofia

F. Oliveira, Susan Wonnacott, Isabel Bermudez, Giovanni Ciccotti, Timothy Gallagher, Richard B. Sessions and Adrian J. Mulholland; Writing of the manuscript: Ana Sofia F. Oliveira, Richard B. Sessions and Adrian J. Mulholland; Review & Editing of the manuscript: Christopher J. Woods, Phil Bates, Susan Wonnacott, Isabel Bermudez, Giovanni Ciccotti, Timothy Gallagher; Funding Acquisition: Phil Bates, Richard B. Sessions, Adrian J. Mulholland and Timothy Gallagher.

References

1. Thompson, A. J.; Lester, H. A.; Lummis, S. C., The structural basis of function in Cys-loop receptors. *Q. Rev. Biophys.* **2010,** *43*, 449-499.
2. Nemecz, A.; Prevost, M. S.; Menny, A.; Corringer, P. J., Emerging Molecular Mechanisms of Signal Transduction in Pentameric Ligand-Gated Ion Channels. *Neuron* **2016,** *90*, 452-470.
3. Changeux, J. P., The nicotinic acetylcholine receptor: a typical 'allosteric machine'. *Philos. Trans. R. Soc. Lond. B Biol. Sci.* **2018,** *373*.
4. Wonnacott, S., Presynaptic nicotinic ACh receptors. *Trends in Neurosci.* **1997,** *20* (2), 92-98.
5. Dineley, K. T.; Pandya, A. A.; Yakel, J. L., Nicotinic ACh receptors as therapeutic targets in CNS disorders. *Trends Pharmacol. Sci.* **2015,** *36*, 96-108.
6. Casida, J.; Berenbaum, M., Neonicotinoids and Other Insect Nicotinic Receptor Competitive Modulators: Progress and Prospects. *Annu. Rev. Entomol.* **2018,** *63*, 125-144.
7. Haydar, S.; Dunlop, J., Neuronal Nicotinic Acetylcholine Receptors - Targets for the Development of Drugs to Treat Cognitive Impairment Associated with Schizophrenia and Alzheimer's Disease. *Cur. Top. Med. Chem.* **2010,** *10* (2), 144-152.
8. Jones, A. S., DB, Diversity of Insect Nicotinic Acetylcholine Receptor Subunits. In *Insect Nicotinic Acetylcholine Receptors. Advances in Experimental Medicine and Biology*, Thany, S., Ed. Springer: New York, 2010; Vol. 683.
9. Miyazawa, A.; Fujiyoshi, Y.; Unwin, N., Structure and gating mechanism of the acetylcholine receptor pore. *Nature* **2003,** *423*, 949-55.
10. Unwin, N., Nicotinic acetylcholine receptor and the structural basis of neuromuscular transmission: insights from Torpedo postsynaptic membranes. *Q. Rev. Biophys.* **2013,** *46*, 283-322.
11. Walsh, R. M., Jr.; Roh, S. H.; Gharpure, A.; Morales-Perez, C. L.; Teng, J.; Hibbs, R. E., Structural principles of distinct assemblies of the human alpha4beta2 nicotinic receptor. *Nature* **2018,** *557*, 261-265.
12. Morales-Perez, C. L.; Noviello, C. M.; Hibbs, R. E., X-ray structure of the human alpha 4 beta 2 nicotinic receptor. *Nature* **2016,** *538*, 411-415.
13. Nys, M.; Kesters, D.; Ulens, C., Structural insights into Cys-loop receptor function and ligand recognition. *Biochem. Pharmacol.* **2013,** *86*, 1042-1053.
14. Dajas-Bailador, F.; Wonnacott, S., Nicotinic acetylcholine receptors and the regulation of neuronal signalling. *Trends Pharmacol. Sci.* **2004,** *25* (6), 317-324.
15. Shen, X. M.; Ohno, K. J.; Tsujino, A.; Brengman, J. M.; Gingold, M.; Sine, S. M.; Engel, A. G., Mutation causing severe myasthenia reveals functional asymmetry of AChR signature cystine loops in agonist binding and gating. *J. Clin. Invest.* **2003,** *111*, 497-505.
16. Kash, T. L.; Jenkins, A.; Kelley, J. C.; Trudell, J. R.; Harrison, N. L., Coupling of agonist binding to channel gating in the GABA(A) receptor. *Nature* **2003,** *421*, 272-275.
17. Bouzat, C.; Gumilar, F.; Spitzmaul, G.; Wang, H.; Rayes, D.; Hansen, S.; Taylor, P.; Sine, S., Coupling of agonist binding to channel gating in an ACh-binding protein linked to an ion channel. *Nature* **2004,** *430* (7002), 896-900.
18. Chakrapani, S.; Bailey, T.; Auerbach, A., Gating dynamics of the acetylcholine receptor extracellular domain. *J. Gen. Physiol.* **2004,** *123* (4), 341-356.
19. Xiu, X.; Hanek, A.; Wang, J.; Lester, H.; Dougherty, D., A unified view of the role of electrostatic interactions in modulating the gating of Cys loop receptors. *J. Biol. Chem.* **2005,** *280* (50), 41655-41666.

20. Lee, W.; Sine, S., Principal pathway coupling agonist binding to channel gating in nicotinic receptors. *Nature* **2005,** *438* (7065), 243-247.
21. Grutter, T.; de Carvalho, L. P.; Dufresne, V.; Taly, A.; Edelstein, S. J.; Changeux, J. P., Molecular tuning of fast gating in pentameric ligand-gated ion channels. *Proc. Natl. Acad. Sci. U. S. A.* **2005,** *102*, 18207-18212.
22. Jha, A.; Cadugan, D. J.; Purohit, P.; Auerbach, A., Acetylcholine receptor gating at extracellular transmembrane domain interface: the cys-loop and M2-M3 linker. *J. Gen. Physiol.* **2007,** *130*, 547-558.
23. Bouzat, C.; Bartos, M.; Corradi, J.; Sine, S., The interface between extracellular and transmembrane domains of homomeric Cys-loop receptors governs open-channel lifetime and rate of desensitization. *J. Neurosci.* **2008,** *28* (31), 7808-7819.
24. Lee, W.; Free, C.; Sine, S., Binding to Gating Transduction in Nicotinic Receptors: Cys-Loop Energetically Couples to Pre-M1 and M2-M3 Regions. *J. Neurosci.* **2009,** *29* (10), 3189-3199.
25. Andersen, N.; Corradi, J.; Bartos, M.; Sine, S.; Bouzat, C., Functional Relationships between Agonist Binding Sites and Coupling Regions of Homomeric Cys-Loop Receptors. *J. Neurosci.* **2011,** *31* (10), 3662-3669.
26. Campos-Caro, A.; Sala, S.; Ballesta, J. J.; Vicente-Agullo, F.; Criado, M.; Sala, F., A single residue in the M2-M3 loop is a major determinant of coupling between binding and gating in neuronal nicotinic receptors. *Proc Natl Acad Sci U S A* **1996,** *93*, 6118-23.
27. Lynch, J.; Rajendra, S.; Pierce, K.; Handford, C.; Barry, P.; Schofield, P., Identification of intracellular and extracellular domains mediating signal transduction in the inhibitory glycine receptor chloride channel. *EMBO J.* **1997,** *16* (1), 110-120.
28. Rovira, J. C.; Ballesta, J. J.; Vicente-Agullo, F.; Campos-Caro, A.; Criado, M.; Sala, F.; Sala, S., A residue in the middle of the M2-M3 loop of the beta4 subunit specifically affects gating of neuronal nicotinic receptors. *FEBS Lett.* **1998,** *433*, 89-92.
29. Rovira, J. C.; Vicente-Agullo, F.; Campos-Caro, A.; Criado, M.; Sala, F.; Sala, S.; Ballesta, J. J., Gating of alpha(3)beta(4) neuronal nicotinic receptor can be controlled by the loop M2-M3 of both alpha(3) and beta(4) subunits. *Pflugers Archiv.* **1999,** *439*, 86-92.
30. Grosman, C.; Salamone, F. N.; Sine, S. M.; Auerbach, A., The extracellular linker of muscle acetylcholine receptor channels is a gating control element. *J. Gen. Physiol.* **2000,** *116*, 327-340.
31. Huggins, D. J.; Biggin, P. C.; Dämgen, M. A.; Essex, J. W.; Harris, S. A.; Henchman, R. H.; Khalid, S.; Kuzmanic, A.; Laughton, C. A.; Michel, J.; Mulholland, A. J.; Rosta, E.; Sansom, M. S. P.; van der Kamp, M. W., Biomolecular simulations: From dynamics and mechanisms to computational assays of biological activity. *WIRES Comput. Mol. Sci.* **2018,** *e1393*, 1-23.
32. Oliveira, A. S. F.; Shoemark, D. K.; Campello, H. R.; Gallagher, T.; Sessions, R. B.; Mulholland, A. J., Identification of the initial steps in signal transduction in the α4β2 nicotinic receptor: insights from equilibrium and nonequilibrium simulations. *Structure* **2019,** *27*, 1171-1183.
33. Jadey, S.; Auerbach, A., An integrated catch-and-hold mechanism activates nicotinic acetylcholine receptors. *J. Gen. Physiol.* **2012,** *140*, 17-28.
34. Purohit, P.; Auerbach, A., Loop C and the mechanism of acetylcholine receptor-channel gating. *J. Gen. Physiol.* **2013,** *141*, 467-478.
35. Pless, S. A.; Sivilotti, L. G., A tale of ligands big and small: An update on how pentameric ligand-gated ion channels interact with agonists and proteins. *Curr. Opin. Physiol.* **2018,** *2*, 19-26.
36. Van Arnam, E. B.; Dougherty, D. A., Functional probes of drug-receptor interactions implicated by structural studies: Cys-loop receptors provide a fertile testing ground. *J. Med. Chem.* **2014,** *57*, 6289-6300.
37. Newell, J. G.; Czajkowski, C., The GABA(A) receptor alpha(1) subunit Pro(174)-Asp(191) segment is involved in GABA binding and channel gating. *J. Biol. Chem.* **2003,** *278*, 13166-13172.
38. Thompson, A. J.; Padgett, C. L.; Lummis, S. C. R., Mutagenesis and molecular modeling reveal the importance of the 5-HT3 receptor F-loop. *J. Biol. Chem.* **2006,** *281*, 16576-16582.
39. Bafna, P. A.; Purohit, P. G.; Auerbach, A., Gating at the mouth of the acetylcholine receptor channel: energetic consequences of mutations in the alphaM2-cap. *PLoS One* **2008,** *3*, e2515.
40. Lee, W. Y.; Free, C. R.; Sine, S. M., Nicotinic receptor interloop proline anchors beta1-beta2 and Cys loops in coupling agonist binding to channel gating. *J. Gen. Physiol.* **2008,** *132*, 265-78.
41. Kusama, T.; Wang, J.; Spivak, C.; Uhl, G., Mutagenesis of the GABA RHO-1 receptor alters agonist affinity and channel gating. *Neuroreport* **1994,** *5* (10), 1209-1212.

42. Lewis, T.; Sivilotti, L.; Colquhoun, D.; Gardiner, R.; Schoepfer, R.; Rees, M., Properties of human glycine receptors containing the hyperekplexia mutation alpha 1(K276E) expressed in Xenopus oocytes. *J. Physiol.-London* **1998,** *507* (1), 25-40.
43. O'Shea, S.; Harrison, N., Arg-274 and Leu-277 of the gamma-aminobutyric acid type A receptor alpha(2) subunit define agonist efficacy and potency. *J. Biol. Chem.* **2000,** *275* (30), 22764-22768.
44. Sigel, E.; Buhr, A.; Baur, R., Role of the conserved lysine residue in the middle of the predicted extracellular loop between M2 and M3 in the GABA(A) receptor. *J. Neurochem.* **1999,** *73* (4), 1758-1764.
45. Deane, C.; Lummis, S., The role and predicted propensity of conserved proline residues in the 5-HT3 receptor. *J. Biol. Chem.* **2001,** *276* (41), 37962-37966.
46. Jensen, M. O.; Park, S.; Tajkhorshid, E.; Schulten, K., Energetics of glycerol conduction through aquaglyceroporin GlpF. *Proc. Natl. Acad. Sci. U. S. A.* **2002,** *99*, 6731-6736.
47. De Fabritiis, G.; Coveney, P. V.; Villa-Freixa, J., Energetics of K+ permeability through Gramicidin A by forward-reverse steered molecular dynamics. *Proteins* **2008,** *73*, 185-194.
48. Ngo, V.; Stefanovski, D.; Haas, S.; Farley, R. A., Non-equilibrium dynamics contribute to ion selectivity in the KcsA channel. *PLoS One* **2014,** *9*, e86079.
49. Ngo, V.; Wang, Y.; Haas, S.; Noskov, S. Y.; Farley, R. A., K+ Block Is the Mechanism of Functional Asymmetry in Bacterial Na(v) Channels. *PLoS Comput. Biol.* **2016,** *12*, e1004482.
50. Ciccotti, G.; Jacucci, G.; McDonald, I. R., Thought-Experiments by Molecular Dynamics. *J. Stat. Phys.* **1979,** *21*, 1-21.
51. Ciccotti, G., Molecular dynamics simulation of non equilibrium phenomena and rare dynamical events. In *Computer simulation in material science*, Meyer M, P. V., Ed. Kluwer Academic Publishers: 1991; pp 119–137.
52. Ciccotti, G.; Ferrario, M., Non-equilibrium by molecular dynamics: a dynamical approach. *Mol. Simul.* **2016,** *42* (16), 1385-1400.
53. Bouzat, C.; Mukhtasimova, N., The nicotinic acetylcholine receptor as a molecular machine for neuromuscular transmission. *Curr. Opin. Physiol.* **2018,** *04*, 40–48.
54. Corringer, P. J.; Poitevin, F.; Prevost, M. S.; Sauguet, L.; Delarue, M.; Changeux, J. P., Structure and pharmacology of pentameric receptor channels: from bacteria to brain. *Structure* **2012,** *20*, 941-956.
55. Newell, J. G.; McDevitt, R. A.; Czajkowski, C., Mutation of glutamate 155 of the GABA(A) receptor beta(2) subunit produces a spontaneously open channel: A trigger for channel activation. *J. Neurosci.* **2004,** *24*, 11226-11235.
56. Padgett, C. L.; Lummis, S. C. R., The F-loop of the GABA(A) receptor gamma(2) subunit contributes to benzodiazepine modulation. *J. Biol. Chem.* **2008,** *283*, 2702-2708.
57. Pless, S. A.; Lynch, J. W., Ligand-specific Conformational Changes in the alpha 1 Glycine Receptor Ligand-binding Domain. *J. Biol. Chem.* **2009,** *284*, 15847-15856.
58. Khatri, A.; Sedelnikova, A.; Weiss, D. S., Structural Rearrangements in Loop F of the GABA Receptor Signal Ligand Binding, Not Channel Activation. *Biophys. J.* **2009,** *96*, 45-55.
59. Eisele, J. L.; Bertrand, S.; Galzi, J. L.; Devillers-Thiery, A.; Changeux, J. P.; Bertrand, D., Chimaeric nicotinic-serotonergic receptor combines distinct ligand binding and channel specificities. *Nature* **1993,** *366*, 479-483.
60. Magnus, C. J.; Lee, P. H.; Atasoy, D.; Su, H. H.; Looger, L. L.; Sternson, S. M., Chemical and genetic engineering of selective ion channel-ligand interactions. *Science* **2011,** *333*, 1292-1296.

TOC graphic

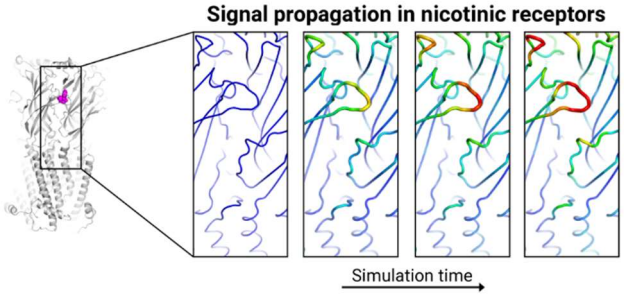
Signal propagation in nicotinic receptors
Simulation time